On the Optimization of InGaAs–InAlAs Quantum-Well Structures for Electroabsorption Modulators

Mauricio Pamplona Pires, Patrícia Lustoza de Souza, Boris Yavich, Ricardo G. Pereira, and Wilson Carvalho, Jr.

***Abstract*—Several InGaAs–InAlAs multiple quantum-well structures grown by metalorganic vapor phase epitaxy (MOVPE), with various Ga content and quantum-well width, have been investigated for electroabsorption modulators (EAM's). The light-hole heavy-hole splitting, the chirp parameter, the insertion loss and the figure of merit $\Gamma\Delta\alpha/F$ of the different InGaAs–InAlAs structures have been evaluated with photocurrent, photoluminescence, absorption and X-ray measurements. It was then possible to experimentally study the influence of different parameters of the multiple quantum-well structures on the device performance. The use of tensile strained barriers are believed to be responsible for the improvement in the figure of merit. Structures with unresolved light-hole and heavy-hole transitions, with negligible chirp, with adequate insertion loss and with extremely high values for $\Gamma\Delta\alpha/F$ have been obtained, however, not simultaneously.**

***Index Terms*—InGaAs–InAlAs, modulators, metalorganic vapor phase epitaxy (MOVPE), quantum-wells.**

I. Introduction

In THE past years, external optical modulators operating at 1.55 μm have drawn much attention from researchers due to their great potential for application in optical communications. External modulation leads to lower chirp compared to direct laser modulation which is advantageous for optical fiber transmission due to the substantial fiber dispersion at 1.55 μm. On the other hand, optical fibers have a minimum attenuation at this wavelength, which largely compensates for the dispersion draw back. The InGaAs–InAlAs multiple quantum-well (MQW) system is of paramount importance for the development of amplitude modulators based on the quantum confined Stark effect [1] for telecommunication applications [2], [3]. This system can produce structures which operate at 1.55 μm, it can be grown on InP substrates for optoelectronic integration and it has a lower valence band offset than the InGaAs–InP system. This last property is desirable to avoid saturation effects due to a long hole escape time from the quantum-wells (QW's) [4]. Nevertheless, if the InGaAs–InAlAs system is expected to be used in the next multigigabit long-haul fiber transmission systems, the MQW structure containing these materials should be further optimized.

When the InGaAs–InAlAs structure is grown lattice-matched to InP, the width of the quantum-well (QW) for operation at 1.55 μm is uniquely defined as 70 Å. However, it is known that the Stark shift should increase with the QW width [5], [6]. On the other hand, wide QW's reduce the overlap between the electron and hole wave-functions [6]. Therefore, optimization of the modulator's MQW structure requires a compromise between the Stark shift and the transition oscillator strength. This compromise can be reached with strained layers and can be probed by the contrast ratio (CR) that is, the ratio between the transmitted signal of the on and off states. The CR is determined by the change in absorption coefficient between the on and off states ($\Delta\alpha$) for a given overlap of the optical mode with the MQW structure (Γ) and modulator length (L) [7], through $\mathrm{CR} = 4.343\Gamma L\Delta\alpha$. However, for high frequency applications it is important to achieve a certain $\Delta\alpha$ with the lowest possible applied voltage. Thus, a figure of merit $\Gamma\Delta\alpha/F$ (dB / 100 μm) / (V / μm), which takes into consideration the electric field (F) needed to reach a certain $\Delta\alpha$ has been proposed [8]. As it will be pointed out in the next paragraph, maximization of this figure of merit alone may not be satisfactory.

Other two crucial parameters in the optimization of the MQW structure for modulators are the light hole-heavy hole splitting (Δs) and the chirp parameter (α_L). The former should be zero for polarization independence of the device and, in theory, for operation at 1.55 μm, it should occur for a 100 Å wide strained InGaAs QW with 0.52 Ga content (0.35% strain) [9]. The latter is defined as $(4\pi/\lambda)(\Delta n/\Delta\alpha)$, where Δn is the change in refractive index and is obtained from $\Delta\alpha$ through the Kramers–Krönig relation [10]. α_L translates the chirp of the modulator, that is, the enhancement of the wavelength linewidth caused by the unavoidable change in refractive index when a change in the absorption coefficient occurs. It should be minimum and it should not exceed the ± 1 range for long distance transmission to guarantee the signal quality.

Polarization insensitive [9], [11], [12], almost chirp-free [13]–[17] InGaAs–InAlAs amplitude modulators and MQW structures with a high $\Gamma\Delta\alpha/F$ figure of merit [11], [12] have already been independently obtained. A simultaneous analysis of all these parameters for operation at 1.55 μm, to the authors knowledge, has not yet been reported. Most of the published work has been performed in MBE grown samples. However, if one is interested in optoelectronic integration on InP substrates, it is desirable to optimize structures for metalorganic

Manuscript received July 27, 1999; revised January 6, 2000. This work was supported by CNPq and Finep.

M. P. Pires, P. L. de Souza, R. G. Pereira, and B. Yavich are with Laboratório de Semicondutores—Centro de Estudos em Telecomunicações, Pontifícia Universidade Católica do Rio de Janeiro, Rio de Janeiro 22453-900, Brazil (e-mail: mauricio@mamao.cetuc.puc-rio.br).

W. Carvalho is with CPqD-Telebrás, LNLS-CNPq, Rodovia Campinas-Mogi Mirim Km 118, Campinas, 13088-061, São Paulo, Brazil.

Publisher Item Identifier S 0733-8724(00)03044-9.

vapor phase epitaxy (MOVPE) growth because it is simpler to fabricate layers containing P with this technique.

In this report, the results of a thorough investigation of MOVPE grown InGaAs–InAlAs MQW structures with various Ga content (x) in the QW alloy and QW width (w) are reported. In optimizing the MQW structures for amplitude modulators, $\Gamma\Delta\alpha/F$, α_L, and Δs were considered. All these parameters were determined using photocurrent (PC), photoluminescence (PL), absorption and X-ray diffraction results, as well as theoretical simulations.

II. Experimental Details

The samples were grown by MOVPE at 100 mbar and at 635°C on n^+ InP substrates. The active region consists of an intrinsic 20 period MQW structure with tensile strained InGaAs QW's with different w and x. The InAlAs barriers are 65 Å thick and they are tensile strained between 0.05 and 0.1%. The MQW structure is inserted between n and p layers, forming a p-i-n diode. The MQW region is separated from the n and p layers by an InAlAs spacer layer of 620 and 2500 Å, respectively, to avoid the diffusion of the dopants into the MQW's. Finally, the structure is topped by a p^+ InGaAs contact layer. Si and Zn are used as the n and p type dopants, respectively. Bulk lattice matched InGaAs and InAlAs samples grown under the same conditions showed a full-width at half-maximum (FWHM) of the 10 K PL spectrum of 1.6 and 12 meV, respectively, confirming the good quality of the samples. Hall effect measurements on these intrinsic bulk samples results in a residual doping concentration equal to 8×10^{14} cm^{-3} and 2×10^{16} cm^{-3} for the InGaAs and the InAlAs, respectively.

PC experiments were performed at room temperature (RT) with conventional lock-in techniques, with a tungsten lamp and a 250-mm spectrometer as the source for monochromatic light. The final spectra were obtained by taking the ratio of the photocurrent signal of the samples and the calibration spectra recorded by a bulk InAs cooled photodiode to eliminate the system response. The absorption setup used the same tungsten lamp for the light source as in the PC experiment. For the PL measurements the samples were excited by the 514 nm of an Ar^+ laser and the signal was detected by a nitrogen cooled Ge photodetector. A double crystal diffractometer was used for X-ray diffraction experiments.

III. Results and Discussion

The electron-heavy hole (e1-hh1) and electron-light hole (e1-lh1) transition energies were calculated by solving the Schrödinger equation using a one band effective mass theory [18] where the physical parameters were interpolated from the values of the binary materials [19]. The strain effects on the band structure were modeled using deformation potential theory [18]. Fig. 1 depicts the results of these calculations, where the solid curve corresponds to the change in w with x so as to maintain the lowest transition energy unchanged. The transition energies involving the hh1 and lh1 will be degenerate (Δs) for certain w and x pairs, represented by the dashed curve. As it will be discussed latter, structures with such parameters may respond equivalently to TE and TM polarizations. The

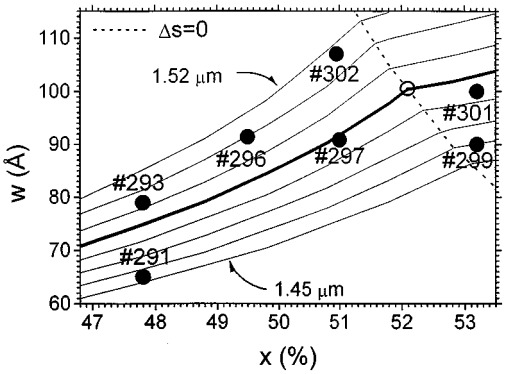

Fig. 1. Well width (w) versus gallium concentration (x) for the lowest transition energy of the quantum-wells. Each line corresponds to a different emission wavelength differing by 10 nm from each other. The lower and upper curves represent the 1.45 μm and the 1.52 μm emission, respectively. The thicker line corresponds to the emission at 1.49 μm. The dotted line represents the well width versus gallium concentration which results in degenerate heavy- and light-hole energies ($\Delta s = 0$). The open circle shows the interception between the curve representing the 1.49 μm emission and the $\Delta s = 0$ curve. The dots represent the investigated samples.

lowest optical transition of samples represented to the left (right) of the dashed curve involve heavy-(light-)holes. The characteristics of an InGaAs–InAlAs MQW structure operating at 1.55 μm, with the transition energy at 1.49 μm (about 30 meV below the lowest MQW transition energy, E1), are represented by the thicker line. It is important to notice that the optimized polarization insensitive InGaAs–InAlAs MQW structure operating at 1.55 μm will have the w and x coordinates depicted in Fig. 1 by the empty dot, where the thicker and dashed curves cross. These calculations are in total agreement with previously reported ones [9]. The solid dots in Fig. 1 represent the investigated samples and the numbers are inserted to help identifying them. The unprocessed samples were first characterized by RT PL. Knowing the transition energy from PL and using the nominal Ga concentration x, it was possible to place the experimental points in Fig. 1. The w of each sample could be evaluated by this procedure. The so determined values of w agree with the X-ray measurements within a 6% error. The observed FWHM of the PL spectra for the MQW were 8 and 25 meV at 10K and RT, respectively, attesting the high quality of the samples. Notice that the different samples were designed to present characteristics which map the x versus w space around the 1.49-μm emission (thicker curve) for x varying from 46.8% (lattice matched) to 53%. This enables one to study the optimization of the modulator in this entire range.

The samples were processed as $180\ \mu\text{m} \times 290\ \mu\text{m}$ photodiodes and were characterized by RT PC with light propagating along the growth axis. The normalized PC spectra at zero bias near the band gap is illustrated for all the samples in Fig. 2. One clearly sees both the (e1-hh1) and (e1-lh1) transitions for samples 291, 293, and 296 (arrows in Fig. 2). These transitions are not resolved for samples 297, 299, 301, and 302 because the hh1 and lh1 energy levels are almost degenerate, as shown in Fig. 1. One observes by comparing Figs. 1 and 2 that the closer the sample position is to the $\Delta s = 0$ curve the more difficult it is to resolve the e1-hh1 and e1-lh1 transitions.

When applying a reverse bias on the samples, the PC spectra are shifted to lower energies. This shift is illustrated for sample

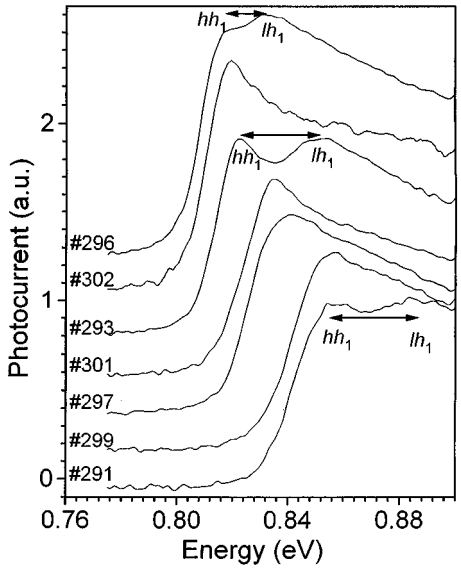

Fig. 2. Room temperature PC spectra of the samples depicted in Fig. 1. The arrows indicate the energy difference between transitions involving the heavy-hole and the light-hole.

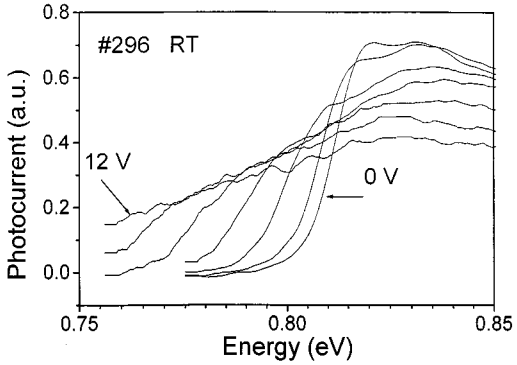

Fig. 3. PC spectra of sample 296 at room temperature for reverse biases from 0–12 V, in steps of 2 V.

296 in Fig. 3. The other samples have a similar behavior, with the magnitude of the Stark shift varying depending on the structure. The PC spectra taken at zero bias is less intense than when bias is applied. Simulations of our diodes' characteristics have proven that this is due to the nonintentional dopant concentration in the InAlAs material (2×10^{16} cm^{-3}). The MQW structure is totally depleted only when subjected to a reverse bias equal to 1.5 V. Therefore, a constant 2-V prereverse bias will from now on be considered. This bias voltage guarantees that all the quantum-wells are depleted. This is in fact usually done since the Stark shift is very small for the first two volts reverse bias. Fig. 4 shows a plot of the Stark shift as a function of the applied electric field evaluated from the PC spectra with different applied reverse bias for samples 291, 297, and 299. The solid lines are a result of the effective mass calculations assuming that the lower transition energy involves the heavy hole. One confirms that the Stark shift is larger, the thicker the quantum well is, as has already been shown [2], [5]. The Stark shift for sample 299 was calculated for both heavy and light hole energy levels, represented in Fig. 4 by the solid and dashed lines, respectively. It is clear that the curve corresponding to the light hole energy

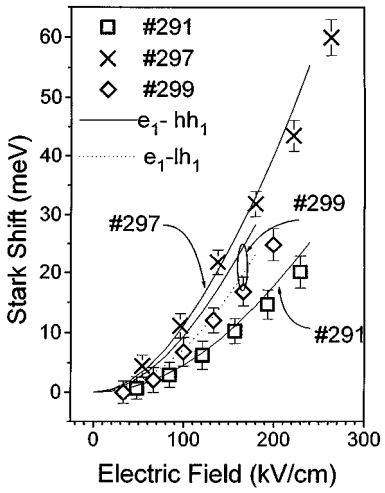

Fig. 4. The Stark shift of samples 291, 297, and 299, with the electric field. The solid (dashed) lines are calculation of the Stark shift of the e1-hh1 (e1-lh1) transition. For sample 299 the light-hole curve fits better the experimental data than the heavy-hole curve does, confirming that the lowest transition energy involves the light hole.

level fits the experimental data better, indicating that the lower transition energy corresponds to the electron-light hole one.

As it has been mentioned before, it is not only the magnitude of the Stark shift that is important for the efficiency of an amplitude modulator, but $\Delta\alpha$, because this parameter takes the overlap of electron and hole wavefunctions into account, as well. The PC spectra qualitatively reveal the absorption characteristics of the sample. However, it is not possible to carry out a quantitative analysis of $\Delta\alpha$ with the normalized PC spectra of Fig. 2 alone. Absorption measurements at zero bias were performed in order to determine the absolute value of the absorption coefficient α, so that a quantitative comparison of the PC spectra for the different samples could be made. The absorption spectra for an energy range near the lowest QW transition (E1) were measured. Assuming that, in the neighborhood of E1, the change in absorption coefficient is essentially due to the MQW structure, it was possible to determine α for each sample at E1 at zero bias. The absorption spectra were obtained by simply multiplying the normalized PC spectra by α of the corresponding sample. The absorption spectra for reverse bias voltages between 4–12 V were subtracted from the one for 2 V prereverse bias, V_0, to generate curves of $\Delta\alpha$ versus energy for different applied voltages, ΔV. Fig. 5 shows $\Delta\alpha$ for each sample as a function of the applied electric field for an energy 30 meV below the RT PL peak at zero bias. The inset of Fig. 5 is a table containing (E1–30 meV) and the residual absorption coefficient at this energy at a reverse bias of 2 V, α_0. Samples 296 and 297 show a larger $\Delta\alpha$ for the measured range of applied electric fields, implying in a better compromise between Stark shift and electron-hole wavefunctions overlap.

Insertion loss due to residual absorption, I_L, is given by $\exp(-\Gamma\alpha_0 L)$ or $(4.434\Gamma\alpha_0 L)$ in dB. Assuming a Γ value equal to 0.1 and a 100 μm long waveguide, I_L at 30 meV below the RT PL peak (the operation wavelength) is calculated for the different samples and the results are shown in Fig. 6, where Fig. 1 was reproduced and the number of the samples were substituted by I_L in dB. Values of I_L up to 2.5 dB are

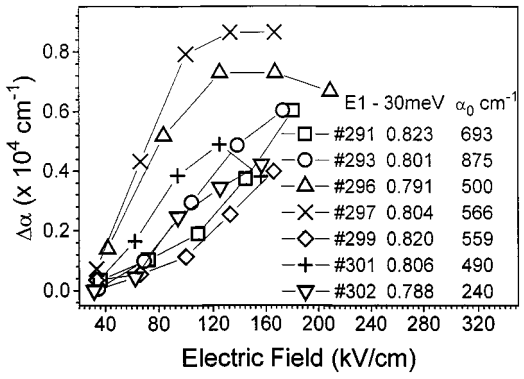

Fig. 5. Determined $\Delta\alpha$ for each sample as a function of the applied electric field. The inset shows the operation energy and the residual absorption coefficient (α_0) at a reverse bias of 2 V.

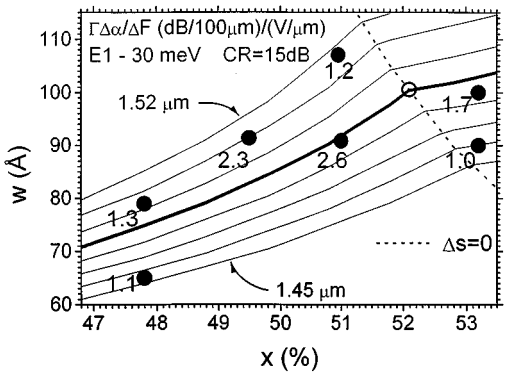

Fig. 7. Reproduction of Fig. 1 where the numbers of the samples were substituted by the figure of merit $\Gamma\Delta\alpha/F$.

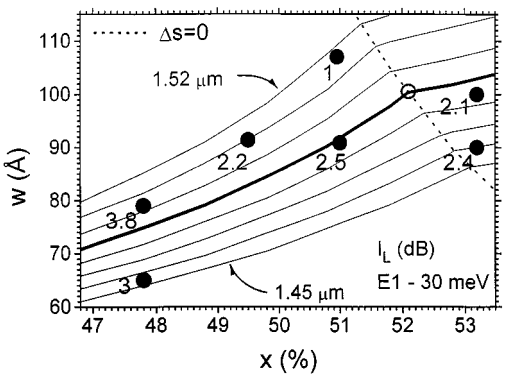

Fig. 6. Reproduction of Fig. 1 where the numbers of the samples were substituted by the insertion loss (I_L).

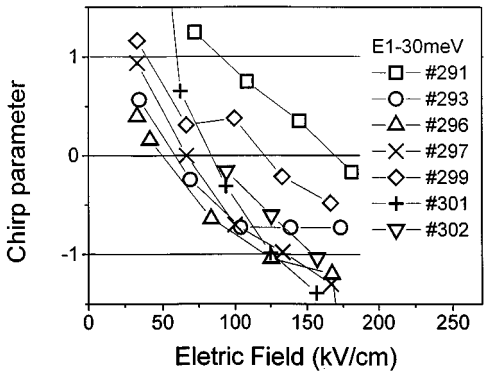

Fig. 8. Chirp parameter (α_L) for energies E_1-30 meV as a function of the electric field. Solid lines are connecting points as a guide for the eyes.

acceptable for amplitude modulators, meaning that all samples except for the ones close to lattice matched are adequate and the thicker sample presents the lowest I_L. On the other hand, the thicker sample does not have such a large $\Delta\alpha$ due to the small overlap between the electron and the hole wavefunctions.

In order to evaluate what electric field should be applied so that a certain $\Delta\alpha$ is attained, and also to be able to compare our results with the available literature, the previously mentioned figure of merit $\Gamma\Delta\alpha/F$ (dB/100 μm)/(V/μm) [8] is calculated at the operation wavelength for a CR equal to 15 dB and Γ equal to 0.1. The same procedure used to construct Fig. 6 was applied to show these results in Fig. 7, where the samples' number were substituted by the corresponding calculated figure of merit. One observes that the thicker sample has a low figure of merit and that samples 296 and 297 have the highest figure of merit. According to the PC spectra shown in Fig. 2, the transitions involving hh1 and lh1 for sample 297 were unresolved, indicating that this sample has essentially degenerate hh1 and lh1 states. The polarization insensitivity of the electroabsorption modulator (EAM) corresponds to an equivalent absorption change with electric field for both the TE and TM modes. The absorption of the TE mode is dominated by the e1-hh1 transition while the absorption for the TM mode is solely due to the e1-lh1 transition. The two crucial parameters responsible for the variation of the absorption spectra with electric field are the overlap of the electron and hole wavefunctions and the Stark shift, which are different for hh and lh. However, according to Chelles *et al.* [11] the change of these two parameters with electric field influences the absorption of TE and TM modes in opposite directions. That is, the overlap increases more rapidly with electric field for the lh1 state while the Stark shift is more pronounced for the hh1 state, resulting in a similar change in the TE and TM modes absorption spectra. Therefore, samples with degenerate hh and lh states, as sample 297, have great potential to produce polarization insensitive devices. Sample 296, which has practically the same well width as sample 297, but a lower x, does not present degenerate hh1 and lh1 states. The low figure of merit for samples 299 and 301, can be explained by the fact that the Stark shift for the light hole level is smaller than that for the heavy hole, as shown in Fig. 4.

The last parameter to be analyzed is the so-called chirp parameter, $a_L = (4\pi\lambda)(\Delta n/\Delta\alpha)$, described in the introduction. Δn was obtained by performing the Kramers–Krönig transform [13] on the PC spectra at different reverse biases for each sample. The results of α_L as a function of applied electric field at the operation wavelength for all samples are depicted in Fig. 8. As it has been mentioned before, α_L should be in the ± 1 range and should be minimum. Comparing α_L at low electric fields for the different samples one observes that α_L is lowest for sample 296. α_L for sample 296 is smaller than that for 297, which has the highest figure of merit and Δs closer to zero, and remains

TABLE I
COMPARISON BETWEEN THE OPERATION WAVELENGTH, λ (μm), INTRINSIC INSERTION LOSS, I_L (dB / 100 μm), OPERATION ELECTRIC FIELD, ΔF (kV/cm), AND THE FIGURE OF MERIT $\Gamma\Delta\alpha/\Delta F$ [(dB / 100 μm)/(V / μm)] FOR A SPECIFIC CONTRAST TO RATIO (15 or 20 dB) OF THE INVESTIGATED SAMPLES AND SAMPLES FROM THE LITERATURE. ALL DATA CONSIDER A 100 μm LONG MODULATOR, EXCEPT WHERE MARKED WITH AN *, WHERE THE MODULATOR SIZE IS SHOWN

Samples	λ	I_L	$\Delta F_{15\,dB}$	$\Delta F_{20\,dB}$	$\Gamma\Delta\alpha_{15\,dB}/\Delta F$	$\Gamma\Delta\alpha_{20\,dB}/\Delta F$
293	1.55	3.8	113	134	1.3	1.5
296	1.57	2.2	64	77	2.3	2.6
297	1.55	2.5	58	69	2.6	2.9
Mitomi *et al.* [21]	1.54	2		250		0.8
Ido *et al.* [9]	1.55	2	87 * (150 μm)		1.3	
Chelles *et al.* [11]	1.58	2	35		4.3	
Wakita *et al.* [12]	1.55	0.5		41 * (200 μm)		2.4

in the ± 1 range for electric fields up to 120 kV/cm. Normally, the optical modulator will be operated with an electric field of the order of 60 kV/cm (Table I). Up to this electric field α_L for sample 296 is negligible and therefore, more suitable for long distance transmission. In fact, for this system there is a compromise between negligible α_L and polarization independence [20]. An experimental evaluation of how α_L changes for InGaAs–InAlAs MQW structures with different QW parameters such as thicknesses and alloy composition has not been reported.

Table I shows a comparison of the results reported here with the ones in the literature. For lattice matched samples, Mitomi *et al.* [21] have reported an optical modulator with an MBE grown InGaAs–InAlAs MQW structure with a figure of merit $\Gamma\Delta\alpha/F_{20\mathrm{dB}}$ (for a CR $=$ 20 dB) of 0.8 (dB / 100 μm)/(V / μm), meanwhile the lattice matched sample (293) operating at 1.55 μm has achieved $\Gamma\Delta\alpha/F = 1.5$ (dB/100 μm)/(V / μm). On the other hand, their structures presented an insertion loss two times lower than the one reported here.

For the strained MQW structures, samples 296 and 297 have presented a value for $\Gamma\Delta\alpha/F_{15\mathrm{dB}}$ two times larger than the previously published results for similar InGaAs–InAlAs structures grown by MBE [3], as shown in Table I. This improvement is most likely due to the characteristics of the barriers. Ido *et al.* in reference [3] have grown barriers which are compressively strained to compensate for the tensile strain of the InGaAs QW. The barriers grown for this investigation are slightly tensile strained. The band offset in this case is larger when compared to the compressively strained case. The larger band offset improves the quantum confinement, and consequently increases the electron and hole wavefunctions overlap, leading to a larger $\Delta\alpha$ for a given applied electric field. In fact, Ido *et al.* [3] have reported a slightly larger Stark shift than the ones measured in this investigation for a similar structure. Thus the larger $\Delta\alpha$, which has been determined in this work, indicates that, for the samples studied, there is a larger overlap in the electron and hole wavefunctions. The slightly larger band offset for the holes will most likely slow down the escape of the holes and may cause problems due to a premature saturation for modulation of high intensity signals [4]. This possibility remains to be verified. In any case, the band offset of the structures containing P in the barriers is still considerably higher than that of lattice matched or tensile strained InAlAs barriers.

Table I shows also results published by Chelles *et al.* [11] who have used strained InGaAs QW's and InAlAs barriers lattice matched to InP grown by MBE. They have claimed a $\Gamma\Delta\alpha/F_{15\mathrm{dB}}$ equal to 4.2 (dB / 100 μm) / (V / μm). One should be careful when comparing this value to the ones reported here because the results of reference [11] were obtained for an operation energy only 15 meV below the lowest optical transition energy. The closer the operation energy is to E1, the lower the required electric field is to achieve a certain CR. This obviously implies in a higher figure of merit. Chelles *et al.* [11] do not report the figure of merit for an operation energy 30 meV below E1 so that a truthful comparison can be made.

All the samples from the literature previously discussed were grown by MBE. The only sample from the literature grown by MOCVD presented on Table I is from Wakita *et al.* [12]. The sample from reference [12] contains intrinsic InGaAsP as stopper layers. The results obtained are very similar to the ones published here, showing a slightly smaller figure of merit but a much better I_L. Such a low I_L may be explained by the fact that they consider 37 meV energy difference between the operation energy and E1.

IV. CONCLUSIONS

A detailed experimental investigation of the optical modulation characteristics of a series of InGaAs–InAlAs MQW structures grown by MOVPE for operation around 1.55 μm was carried out. It was shown that QW widths around 90 Å with x around 50% optimize the figure of merit $\Gamma\Delta\alpha/F$, while the insertion losses due to residual absorption are minimized for thicker QW's. A Ga content in the range between 51–52.5% for the 90 Å thick QW's are required for polarization insensitivity. The chirp parameter can reach an undesirable high value at electric fields below 50 kV/cm for such a structure. On the other hand, for the same w, a negligible chirp was evaluated for an InGaAs QW with 49.5% x. Very high values of the figure of merit $\Gamma\Delta\alpha/F$ for operation at 1.55 μm (0.80 eV), with QW structures whose lowest optical transition wavelength equals 1.49 μm (0.83 eV), using tensile strained InAlAs barriers were obtained. These results also demonstrate the possibility of achieving highly efficient and competitive optical modulation

characteristics with InGaAs–InAlAs MQW structures grown by MOVPE which is recommended for optoelectronic integration.

REFERENCES

[1] Schmitt-Rink, D. S. Chemla, and D. A. Miller, "Linear and nonlinear optical properties of semiconductors quantum wells," *Adv. Phys.*, vol. 38, pp. 89–188, Mar. 1989.

[2] K. Wakita and I. Kotaka, "Multiple-quantum-well optical modulators and their monolithic integration with DFB lasers for optical-fiber communications," *Microwave Opt. Technol. Lett.*, vol. 7, pp. 120–128, Feb. 1994.

[3] T. Ido, S. Tanaka, M. Suzuki, M. Koizumi, H. Sano, and H. Inoue, "Ultra-high-speed multiple-quantum-well electro-absorptive optical modulator with integrated waveguides," *J. Lightwave Technol.*, vol. 14, p. 2026, Dec. 1996.

[4] T. H. Wood, J. Z. Pastralan, C. A. Burrus Jr., B. C. Johnson, B. I. Miller, J. L. de Miguel, U. Koren, and M. G. Young, "Electric field screening by photogenerated holes in multiple quantum wells: A new mechanism for absorption saturation," *Appl. Phys. Lett.*, vol. 57, pp. 1081–1083, Sept. 1990.

[5] G. Bastard, E. Mendez, L. Chang, and L. Esaki, "Variational calculations on a quantum well in a electric field," *Phys. Rev. B*, vol. 28, pp. 3241–3245, Sept. 1983.

[6] R. W. Martin, S. L. Wong, R. J. Nicholas, K. Satzke, M. Gibbon, and E. J. Thrush, "The design of quantum-confined Stark effect modulators for integration with 1.55 μm lasers," *Semicond. Sci. Technol.*, vol. 8, pp. 1173–1178, Apr. 1993.

[7] M. K. Chin and W. S. C. Chang, "Theoretical design optimization of multiple quantum-well electroabsorption waveguide modulators," *IEEE J. Quantum Electron.*, vol. 29, pp. 2476–2487, Sept. 1993.

[8] E. Bigan, M. Allovon, M. Carrè, C. Braud, A. Carenco, and P. Voisin, "Optimization of optical waveguide modulators based on the Wannier–Stark localization: An experimental study," *IEEE J. Quantum Electron.*, vol. 28, pp. 214–233, Jan. 1992.

[9] T. Ido, H. Sano, S. Tanaka, D. J. Moss, and H. Inoue, "Performance of strained InGaAs/InAlas multiple-quantum-well electroabsorption modulators," *J.Lightwave Technol.*, vol. 14, pp. 2324–2331, Oct. 1996.

[10] C. H. Henry, R. A. Logan, and K. A. Bertness, "Spactral dependence of the change in refractive index due to carrier injection in GaAs lasers," *J. Appl. Phys.*, vol. 52, pp. 4457–4461, July 1981.

[11] S. Chelles, R. Ferreira, P. Voisin, and J. C. Harm, "High performance polarization insensitive electroabsorption modulator based on strained GaInAs-AlInAs multiple quantum wells," *Appl. Phys. Lett.*, vol. 67, pp. 247–249, July 1995.

[12] K. Wakita, I. Kotaka, K. Yoshino, S. Kondo, and Y. Noguchi, "Polarization independent electroabsorption modulators using strain-compensated InGaAs-InAlAs MQW structures," *IEEE Photon. Technol. Lett.*, vol. 7, pp. 1418–1420, Dec. 1995.

[13] T. Yamanaka, K. Wakita, and K. Yokoyama, "Potential chirp-free characteristics (negative chirp parameter) in electroabsorption modulators using a wide tensile-strained quantum well structure," *Appl. Phys. Lett.*, vol. 68, pp. 3114–3116, May 1996.

[14] K. Wakita, I. Kotaka, O. Motomi, H. Asai, and Y. Kawamura, "Observation of low-chirp modulation in InGaAs-InAlAs multiple-quantum-well optical modulators under 30 GHz," *IEEE Photon. Technol. Lett.*, vol. 3, pp. 138–140, Feb. 1991.

[15] T. Yamanaka, K. Wakita, and K. Yokoyama, "Pure strained effect on reducing the chirp parameter in InGaAsP/InP quantum well electroabsorption modulators," *Appl. Phys. Lett.*, vol. 70, pp. 87–89, Jan. 1997.

[16] M. Matsuda, K. Morito, K. Yamaji, T. Fujii, and Y. Kotaki, "A novel method for designing chirp characteristics in electroabsorption MQW optical modulators," *IEEE Photon. Technol. Lett.*, vol. 10, pp. 364–366, Mar. 1998.

[17] H. Q. Hou and T. Y. Chang, "Nearly chirp-free electroabsorption modulation using InGaAs-InGaAlAs-InAsAs coupled quantum wells," *IEEE Photon. Technol. Lett.*, vol. 7, pp. 167–169, Feb. 1995.

[18] S. L. Chuang, *Physics of Optoeletronic Devices*. New York: Wiley, 1995.

[19] W. Nakwaski, "Effective masses of electrons and heavy holes in GaAs, InAs, AlAs and their ternary compound," *Physica B*, vol. 210, pp. 1–25, Jan. 1995.

[20] M. Pamplona Pires, B. Yavish, and P. L. Souza, "Chirp dependence in InGaAs/InAlAs multiple quantum well electro-absorptive modulators near polarization-independent condition," *Appl. Phys. Lett.*, vol. 72, pp. 271–273, July 1999.

[21] O. Mitomi, I. Kataka, K. Wakita, S. Nojima, K. Kawano, Y. Kawamura, and H. Asai, "40 GHz bandwidth InGaAs/InAlAs multiple quantum well optical intensity modulators," *Appl. Opt.*, vol. 31, pp. 2030–2035, Apr. 1992.

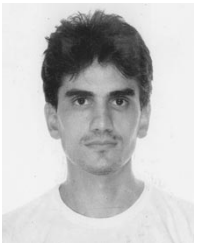

Mauricio Pamplona Pires was born in Salvador, Bahia, Brazil, on January 1, 1969. He received the Bachelor, Master, and Doctor degrees in physics from the Pontifícia Universidade Católica do Rio de Janeiro, PUC-Rio,Brazil, in 1990, 1993, and 1998, respectively.

In 1998, he joined the Center for Telecommunication Studies in PUC-Rio, CETUC, as a Postdoctoral, where he is responsible for the fabrication and optical characterization of optoelectronic semiconductor devices.

Patrícia Lustoza de Souza was born in Curitiba, PR, Brazil, on January 5, 1959. She received the B.A., M.Sc., and Doctor degrees in physics from the University of California, San Diego, in 1981, from the San Diego State University in 1984 and from Pontifícia Universidade Católica do Rio de Janeiro in 1989, respectively.

In 1989, she joined the Pontifcia Universidade Católica do Rio de Janeiro as an Assistant Professor in the Physics Department. In 1991, she moved to the Center for Telecommunication Studies in the same university, where she is now an Associate Professor and Head of the Semiconductor Laboratory. She has been engaged in research in III–V semiconductor materials for electronic and optoelectronic devices, in particular, for optical communication.

Boris Yavich was born in Leningrad, Russia. He received the M.S. degree in metallurgical engineering in 1965 from Leningrad Polytechnic Institute (now St. Petersburg Technical University) and the Ph.D. degree in solid-state physics in 1975 from the Ioffe Physical Technical Institute.

He joined the Ioffe Physical Technical Institute, Leningrad (now St. Petersburg), Russia, in 1965, where he was engaged in research and development of CVD and MOVPE methods for growing Si, Ge and compound semiconductors. His work has involved growth, characterization, design and fabrication of heterojunction photodetectors, solar cells, lasers, photoemitters on the base InGaAs–InAlAs and GaAs–AlGaAs quantum-well structures. He is currently a Senior Scientist in the Department of Physics of Semiconductor Heterostructures. From 1989 to 1993, he was also Associated Professor of Technical University, St. Petersburg. Since 1993, he has been a Visiting Research Scientist at the Center for Telecommunications Studies in the Pontifícia Universidade Católica do Rio de Janeiro (PUC-Rio), Brazil. Much of his work has been on the MOVPE growth of quantum-well structures for 1.55 μm electroabsorbing optical modulator.

Ricardo G. Pereira, photograph and biography not available at the time of publication.

Wilson de Carvalho, Jr. was born in Araraquara, Brazil, on February 8, 1957. He received the B.S. and M.S. degrees in physics from Universidade Federal do Parana and Unicamp in 1980 and 1984, respectively.

In 1984, he joined the TELEBRAS Research and Development Center for Telecommunication, where he has been working on the crystal growth of III–V compounds for optoelectronic applications.

Dr. de Carvalho is member of Brazilian Society of Physics and Brazilian Society of Crystal Growth.